Elasto-viscoplastic consistent tangent operator concept-based implicit boundary element methods*

LIU Yong (刘 勇)[1], Glaucio H. Paulino[2] & LIANG Lihua (梁利华)[3]

1. Institute of Superplasticity and Plasticity, Zhejiang University of Technology, Hangzhou 310014, China;
2. Department of Civil and Env. Eng., University of California, Davis, CA95616-5294, USA;
3. Department of Mechanical Engineering, Zhejiang University of Technology, Hangzhou 310014, China
Correspondence should be addressed to Liang Lihua (email: lyyjs@mail.hz.zj.cn)

Received June 28, 1999

Abstract An elasto-viscoplastic consistent tangent operator (CTO) concept-based implicit algorithm for nonlinear boundary element methods is presented. Both kinematic and isotropic strain hardening are considered. The elasto-viscoplastic radial return algorithm (RRA) and the elasto-viscoplastic CTO and its related scheme are developed. In addition, the limit cases (e.g. elastoplastic problem) of viscoplastic RRA and CTO are discussed. Finally, numerical examples, which are compared with the latest FEM results of Ibrahimbegovic et al. and ABAQUS results, are provided.

Keywords: **boundary element method, elasto-viscoplasticity, consistent tangent operator (CTO), implicit algorithm, computational mechanics.**

Since Simo and Taylor[1] first proposed the use of the consistent tangent operator (CTO) within the context of the elastoplastic finite element method (FEM), the CTO concept has been widely used in various FEM applications[2—5]. It should be indicated that in the recent work of Ibrahimbegovic et al.[5], classical plasticity and viscoplasticity models were further reformulated for BEM based on the work of Simo and Taylor. In 1996, Bonnet and Mukherjee developed for the first time the CTO in an implicit BEM for elastoplasticity[6], but their code and examples are only suitable for one-dimensional problem. Later on Mukherjee and co-workers extended the work for 2D elastoplastic problems with isotropic hardening[7,8]. The results obtained are accurate as compared with analytical solutions and the FEM code ABAQUS. Recently, Paulino and Liu presented a comparison of both consistent and continuum tangent operators for the elastoplastic BEM[9], and have shown by means of numerical examples, the superiority of the consistent over the continuum operator. As compared with the CTO scheme, use of the continuum operator leads to the loss of the quadratic rate of asymptotic convergence which characterizes Newton's iteration method. This represents both more iteration steps and CPU time. However, all the previous work on CTO BEM was based on pure elastoplastic deformation (i.e. rate independent), the elasto-viscoplastic CTO BEM has not yet been studied. When viscoplastic deformation happens, the stress status in the nonlinear region is allowed to exceed the loading surface, and the deformation becomes more complicated as compared with elastoplasticity. This is the basic difference between elasto-viscoplasticity and plasticity.

This paper investigates the viscoplastic problem with a viscoplastic CTO concept-based implicit BEM scheme. The aim is to develop CTO BEM for the elasto-viscoplasticity. First, the ba-

sic implicit algorithm and the formulations of classical elasto-viscoplastic problem are introduced. Second, the elasto-viscoplastic RRA and CTO as well as their limit case are further investigated and discussed. Then the elasto-viscoplastic CTO-based BEM and related scheme with the numerical examples are presented.

1 Basic formulation

1.1 The generalized implicit rule

Let h be a smooth function, and consider the initial value problem

$$\dot{\boldsymbol{x}} = h(\boldsymbol{x}(t)),\ \boldsymbol{x}(0) = \boldsymbol{x}_n;\ t \in [0,T]. \tag{1}$$

We shall be concerned with the following one parameter class of integration algorithms which is referred to as the generalized implicit rule:

$$\begin{cases} \boldsymbol{x}_{n+1} = \boldsymbol{x}_n + \Delta t \cdot h(\boldsymbol{x}_{n+\theta}), \\ \boldsymbol{x}_{n+\theta} = \theta \cdot \boldsymbol{x}_{n+1} + (1-\theta)\boldsymbol{x}_n, \end{cases} \quad \theta \in [0,1], \tag{2}$$

where $\boldsymbol{x}_{n+1} \cong \boldsymbol{x}(t_{n+1})$ denotes the algorithmic approximation to the exact values $\boldsymbol{x}(t_{n+1})$ at time $t_{n+1} = t_n + \Delta t$. This family of algorithm contains well-known implicit integration schemes: in particular, $\theta = 0$ represents explicit (forward Euler) scheme, $\theta = 0.5$ is the so-called midpoint rule, and $\theta = 1$ stands for the implicit (backward Euler) algorithm.

1.2 Implicit viscoplastic problem

In classical formulations of viscoplasticity, the yield criterion is defined through a loading function $f \equiv f(\boldsymbol{\sigma}, \boldsymbol{q})$, where $\boldsymbol{\sigma}$ denotes the stress state and $\boldsymbol{q}$ denotes the internal variables. As elasto-viscoplastic deformation appears, the stress is permissible outside the closure of the loading surface, i.e.

$$f(\boldsymbol{\sigma}, \boldsymbol{q}) > 0. \tag{3}$$

However, in elastoplasticity, $f(\boldsymbol{\sigma}, \boldsymbol{q}) \leqslant 0$, which is the basic difference between viscoplasticity and rate-independent plasticity.

The evolution equations for elasto-viscoplastic problem are formulated in terms of Perzyna's[10] model:

$$\begin{cases} \dot{\boldsymbol{\varepsilon}}^{\mathrm{vp}} = \dot{\gamma}\dfrac{\partial f(\boldsymbol{\sigma}, \boldsymbol{q})}{\partial \boldsymbol{\sigma}}, \\ \dot{\boldsymbol{q}} = -\dot{\gamma}\boldsymbol{D}\dfrac{\partial f(\boldsymbol{\sigma}, \boldsymbol{q})}{\partial \boldsymbol{q}}, \\ \dot{\gamma} = \dfrac{\langle g(f(\boldsymbol{\sigma}, \boldsymbol{q}))\rangle}{\eta}, \end{cases} \tag{4}$$

where $\dot{\gamma}$ is the viscoplastic flow rate parameter, $\boldsymbol{D}$ is the matrix of generalized viscoplastic hardening moduli, $g(x)$ is a monotone function with $g(x) = 0$, if and only if $x \leqslant 0$. $\langle x \rangle = (x + |x|)/2$ is a ramp function, $\eta \in (0, \infty)$ is a given viscoplastic material fluidity parameter. Furthermore, without loss of generality let $g(x) = x$. For metals, typical choices for the function g are exponential and power laws.

The local constitutive equation for rate dependent viscoplasticity, on the other hand, describes the elastic response

$$\dot{\boldsymbol{\sigma}} = \boldsymbol{C} : (\dot{\boldsymbol{\varepsilon}} - \dot{\boldsymbol{\varepsilon}}^{\mathrm{vp}}), \tag{5}$$

where $\boldsymbol{C}$ is the fourth-order tensor of elastic coefficients, : is the natural (Euclidean) inner product. If one considers the limit case of the viscoplastic fluidity parameter in eqs. (4) and (5) as

$\eta \to 0$, one would expect to recover the rate-independent plasticity formulation, i.e. as $\eta \to 0$, states outside the loading surface become increasingly penalized and thus $f \to 0$ in such a way that $\frac{\langle g(f) \rangle}{\eta} \to \dot{\gamma}$ (finite). In this case, the viscoplastic equations (4) and (5) reduce to the rate-independent plastic problem. As the fluidity parameter $\eta \to \infty$, $\dot{\gamma} = \frac{\langle g(f) \rangle}{\eta} \to 0$, $\dot{\boldsymbol{q}} \to 0$, $\dot{\boldsymbol{\varepsilon}}^{\mathrm{vp}} \to 0$, eq. (5) collapses to the rate form of linear elasticity.

2 The viscoplastic consistent tangent operator (CTO)

2.1 Elasto-viscoplastic RRA

Let $\boldsymbol{u}$, $\boldsymbol{\sigma}$ and $\boldsymbol{\varepsilon}$ denote respectively the displacement, stress tensor and total strain tensor. Following Simo and Taylor[1] and considering the evolution problem for strain increment in any given finite time step Δt, the elasto-viscoplastic constitutive law reduces to giving a radial return algorithm rule which makes $\boldsymbol{\sigma}_{n+1}$ finally consistent with $f(\boldsymbol{\sigma}, \boldsymbol{q})$:

$$\boldsymbol{\sigma}_{n+1} = \bar{\boldsymbol{\sigma}}(\boldsymbol{\varepsilon}_n, \boldsymbol{\sigma}_n, \boldsymbol{q}_n, \Delta\boldsymbol{\varepsilon}_n), \tag{6}$$

where the notation $\bar{\boldsymbol{\sigma}}$ symbolically denotes the action of the radial return algorithm (RRA); the internal variables $\boldsymbol{q} = \{\bar{e}^{\mathrm{vp}}, \boldsymbol{\alpha}\}$, in which $\boldsymbol{\alpha}$ stands for back stress; $\bar{e}^{\mathrm{vp}}$ is the cumulated equivalent viscoplastic strain:

$$\bar{e}^{\mathrm{vp}} = \int_0^t \sqrt{\frac{2}{3}} (\dot{\boldsymbol{\varepsilon}}^{\mathrm{vp}} : \dot{\boldsymbol{\varepsilon}}^{\mathrm{vp}}) \mathrm{d}\tau, \tag{7}$$

where the viscoplastic strain rate $\dot{\boldsymbol{\varepsilon}}^{\mathrm{vp}}$ can be written as

$$\dot{\boldsymbol{\varepsilon}}^{\mathrm{vp}} = \dot{\gamma} \frac{\partial f}{\partial \boldsymbol{\sigma}} = \dot{\gamma} \hat{\boldsymbol{n}}, \tag{8}$$

in which $\hat{\boldsymbol{n}}$ is the unit vector normal to the yield surface, with $\mathrm{tr}(\dot{\boldsymbol{\varepsilon}}^{\mathrm{vp}}) = 0$.

The Von-Mises yield condition is

$$f(\boldsymbol{\xi}, \kappa, \boldsymbol{\alpha}) \equiv \| \boldsymbol{\xi} \| - \sqrt{\frac{2}{3}} \kappa(\bar{e}^{\mathrm{vp}}), \tag{9}$$

where $\boldsymbol{\xi} = \boldsymbol{S} - \boldsymbol{\alpha}$ stands for the deviatoric stress $\boldsymbol{S} = \boldsymbol{\sigma} - \frac{1}{3}(\mathrm{tr}\boldsymbol{\sigma})\boldsymbol{I}$; $\boldsymbol{I}$ is the second order unit tensor given by $\boldsymbol{I} = \delta_{ij} \boldsymbol{e}_i \otimes \boldsymbol{e}_j$, where $\boldsymbol{e}_i$ represents the basis vectors and $\otimes$ denotes the tensor product. Also, $\bar{e}^{\mathrm{vp}} \to \kappa(\bar{e}^{\mathrm{vp}})$ is the hardening rule.

A trial (Tr) deviatoric stress is introduced as

$$\boldsymbol{\xi}_{n+1}^{\mathrm{Tr}} = \boldsymbol{S}_n + 2G\Delta\boldsymbol{e}_n - \boldsymbol{\alpha}_n, \tag{10}$$

where $\boldsymbol{e} = \boldsymbol{\varepsilon} - \frac{1}{3}(\mathrm{tr}\boldsymbol{\varepsilon})\boldsymbol{I}$ and G is the shear modulus.

If $f(\boldsymbol{\xi}_{n+1}^{\mathrm{Tr}}, \kappa_n, \boldsymbol{\alpha}_n) = \| \boldsymbol{\xi}_{n+1}^{\mathrm{Tr}} \| - \sqrt{\frac{2}{3}} \kappa(\bar{e}_n^{\mathrm{vp}}) \leqslant 0$, i.e. the elastic deformation, one has

$$\boldsymbol{\sigma}_{n+1} = \bar{\boldsymbol{\sigma}} = K\Delta\boldsymbol{\varepsilon}_n : (\boldsymbol{I} \otimes \boldsymbol{I}) + 2G\Delta\boldsymbol{e}_n + \boldsymbol{\sigma}_n, \tag{11}$$

where K is the bulk modulus. This is the elastic constitutive equation in incremental form. If $f(\boldsymbol{\xi}_{n+1}^{\mathrm{Tr}}, \kappa_n, \boldsymbol{\alpha}_n) > 0$, i.e. the viscoplastic deformation happens, $\bar{\boldsymbol{\sigma}}$ becomes

$$\boldsymbol{\sigma}_{n+1} = \bar{\boldsymbol{\sigma}} = K\boldsymbol{\varepsilon}_{n+1} : (\boldsymbol{I} \otimes \boldsymbol{I}) + \boldsymbol{S}_{n+1}, \tag{12}$$

where $\boldsymbol{S}_{n+1} = \boldsymbol{\alpha}_n + \sqrt{\frac{2}{3}} \left(\kappa + \sqrt{\frac{3}{2}} f + \sqrt{\frac{2}{3}} H'[\dot{\gamma}\Delta t] \right) \hat{\boldsymbol{n}}$, $H = H(\bar{e}^{\mathrm{vp}})$, $H(\bar{e}^{\mathrm{vp}})$ is the plastic

modulus which characterizes the kinematic hardening response. Here, a superposed "prime" represents differentiation with respect to the argument.

On the other hand, from eqs. (2), (4)—(9), and letting $\theta = 1$ in eq. (2), one can obtain the following counterpart of the implicit backward-Euler difference scheme and viscoplastic RRA consistency equations

$$\begin{cases} \dot{\boldsymbol{\varepsilon}}^{\mathrm{vp}} = \dot{\gamma}\dfrac{\partial f(\boldsymbol{\sigma},\boldsymbol{q})}{\partial \boldsymbol{\sigma}} = \dfrac{\langle f(\boldsymbol{\sigma},\boldsymbol{q})\rangle}{\eta}\hat{\boldsymbol{n}}, \\ \boldsymbol{\varepsilon}^{\mathrm{vp}}_{n+1} = \boldsymbol{\varepsilon}^{\mathrm{vp}}_{n} + \dfrac{f_{n+1}}{\eta}\Delta t\,\hat{\boldsymbol{n}}, \\ \boldsymbol{\alpha}_{n+1} = \boldsymbol{\alpha}_{n} + \dfrac{2}{3}H'[\dot{\gamma}\Delta t]\hat{\boldsymbol{n}}, \\ \bar{e}^{\mathrm{vp}}_{n+1} = \bar{e}^{\mathrm{vp}}_{n} + \sqrt{\dfrac{2}{3}}[\dot{\gamma}\Delta t], \\ \hat{\boldsymbol{n}} = \dfrac{1}{\| \boldsymbol{\xi}^{\mathrm{Tr}} \|}\boldsymbol{\xi}^{\mathrm{Tr}}_{n+1}, \end{cases} \tag{13}$$

along with the condition

$$\| \boldsymbol{\xi}_{n+1} \| = \| \boldsymbol{\xi}^{(\mathrm{Tr})}_{n+1} \| - 2G[\dot{\gamma}\Delta t]\left(1 + \frac{1}{3G}H'\right). \tag{14}$$

From eq. (14) it further follows that

$$[\dot{\gamma}\Delta t] = \frac{\langle f_{n+1}\rangle \Delta t}{\eta} = \frac{f^{\mathrm{Tr}}/2G}{1 + \dfrac{H'}{3G} + \dfrac{\eta}{2G\Delta t}}, \tag{15}$$

where f^{Tr} is the trial yield function.

Eq. (15) and Von-Mises yield condition (9) solve the viscoplastic consistency equation:

$$\Psi(\dot{\gamma}\Delta t) \equiv \| \boldsymbol{\xi}^{\mathrm{Tr}}_{n+1} \| - \sqrt{\frac{2}{3}}\boldsymbol{\kappa}(\bar{e}^{\mathrm{vp}}_{n} + \sqrt{\frac{2}{3}}[\dot{\gamma}\Delta T]) - 2G[\dot{\gamma}\Delta t]\left(1 + \frac{H'}{3G} + \frac{\eta}{2G\Delta t}\right) = 0 \tag{16}$$

with $\boldsymbol{\kappa} = \boldsymbol{\kappa}(\bar{e}^{\mathrm{vp}}_{n+1})$, $H' = H'(\bar{e}^{\mathrm{vp}}_{n+1})$.

From eq. (15), one observes that

$$[\dot{\gamma}\Delta t] = \frac{\langle f_{n+1}\rangle \Delta t}{\eta} \to \frac{f^{\mathrm{Tr}}}{2G(1 + H'/3G)}, \quad \text{as } \frac{\eta}{\Delta t} \to 0, \tag{17}$$

i.e. eq. (15) reduces to the rate independent plastic case eq. (17). This illustrates the fact that as $\eta \to 0$ one recovers the rate independent plasticity[2]. Particularly, eq. (16) at this case is in agreement with the plasticity consistency equation, which agrees with the results of Bonnet and Mukherjee[6]. The solution of eq. (16) from which the converged values of $[\dot{\gamma}\Delta t]$ is determined can be effectively accomplished by the local Newton iteration procedure. An illustration of RRA is given in fig. 1, where the actions take place on $\kappa(\bar{e}^{\mathrm{vp}})$.

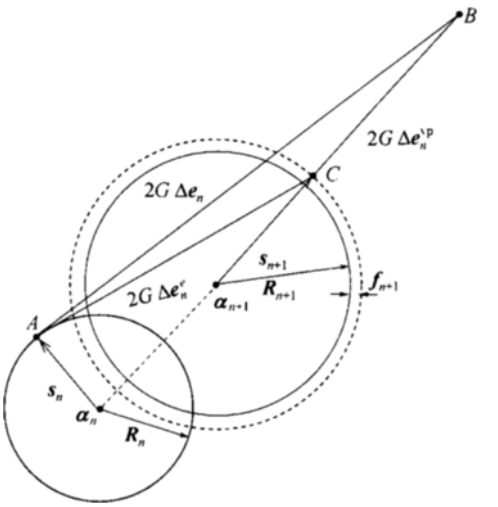

Fig. 1. Illustration of the radial return algorithm (RRA) with both kinematic and isotropic hardening ($R = \sqrt{\frac{2}{3}}\cdot$ $\kappa(\bar{e}^{\mathrm{vp}})$).

the π-plane which illustrates a general viscoplastic case with isotropic and kinematic hardening. Note that as $\eta \to 0$, $f_{n+1} \to 0$, and it actually returns to the elasto-plastic case.

The viscoplastic RRA scheme is summarized below:

(i) Compute trial elastic stress: $\boldsymbol{\xi}_{n+1}^{\mathrm{Tr}} = \boldsymbol{S}_n + 2G\Delta \boldsymbol{e}_{n+1} - \boldsymbol{\alpha}_n$.

(ii) Compute unit normal field: $\hat{\boldsymbol{n}} = \dfrac{\boldsymbol{\xi}_{n+1}^{\mathrm{Tr}}}{\| \boldsymbol{\xi}_{n+1}^{\mathrm{Tr}} \|}$.

(iii) Use the above converged value of $[\dot{\gamma}\Delta t]$ to compute the equivalent viscoplastic strain: $\bar{e}_{n+1}^{\mathrm{vp}} = \bar{e}_n^{\mathrm{vp}} + \sqrt{\dfrac{2}{3}}[\dot{\gamma}\Delta t]$ and the back stress $\boldsymbol{\alpha}_{n+1} = \boldsymbol{\alpha}_n + \dfrac{2}{3}H'[\dot{\gamma}\Delta t]\hat{\boldsymbol{n}}$.

(iv) Compute the deviatoric stress: $\boldsymbol{S}_{n+1} = \left(f_{n+1} + \sqrt{\dfrac{2}{3}}\kappa(\bar{e}_{n+1}^{\mathrm{vp}})\right)\hat{\boldsymbol{n}} + \boldsymbol{\alpha}_{n+1}$.

(v) Compute: $\boldsymbol{\sigma}_{n+1} = K\boldsymbol{\varepsilon}_{n+1} : (\boldsymbol{I} \otimes \boldsymbol{I}) + \boldsymbol{S}_{n+1}$.

It should be indicated that if the trial stress $\boldsymbol{\xi}_{n+1}^{\mathrm{Tr}(i)}$ and the final stress $\boldsymbol{\sigma}_{n+1}^{(i)}$ at the ith iteration are computed from the nonconverged stress $\boldsymbol{S}_{n+1}^{(i-1)}$ at the previous iteration (rather than from converged stress $\boldsymbol{S}_n$ as above), then the continuum viscoplastic tangent operator is obtained from the general scheme of CTO.

2.2 Elasto-viscoplastic CTO

The CTO, which is defined in a fourth order tensor[1,6]

$$\boldsymbol{C}_{n+1} = \frac{\partial \boldsymbol{\sigma}_{n+1}}{\partial \Delta \boldsymbol{\varepsilon}_n}, \tag{18}$$

which depends on the particular algorithm $\delta\boldsymbol{\varepsilon}_n \to \boldsymbol{\sigma}_{n+1}(\boldsymbol{\varepsilon}_n, \boldsymbol{\sigma}_n, \boldsymbol{q}_n, \Delta\boldsymbol{\varepsilon}_n)$ chosen. For the RRA presented here, neglecting the deriving process, the CTO takes the form

$$\boldsymbol{C}_{n+1} = \boldsymbol{C}_{n+1}^{\mathrm{vp}} = K\boldsymbol{I} \otimes \boldsymbol{I} + 2G\beta\left(\boldsymbol{I} - \frac{1}{3}\boldsymbol{I} \otimes \boldsymbol{I}\right) - 2G\bar{\gamma}\hat{\boldsymbol{n}} \otimes \hat{\boldsymbol{n}}, \tag{19}$$

where

$$\beta = 1 - \frac{2G[\dot{\gamma}\Delta t]}{\| \boldsymbol{\xi}_{n+1}^{\mathrm{Tr}} \|}, \quad \bar{\gamma} = \frac{1}{\dfrac{\eta}{2G\Delta t} + 1 + \dfrac{K' + H'}{3G}} - (1 - \beta),$$

$$\boldsymbol{I} = (1/2)[\delta_{ik}\delta_{jl} + \delta_{il}\delta_{jk}]\boldsymbol{e}_i \otimes \boldsymbol{e}_j \otimes \boldsymbol{e}_k \otimes \boldsymbol{e}_l.$$

In the above equation, when $\dfrac{\eta}{2G\Delta t} \to 0$, the purely plastic CTO is recovered. When $\beta = 1.0$ and $[\dot{\gamma}\Delta t]$ does not guarantee to take the converged value, the viscoplastic continuum tangent operator (CTO) is obtained. Its expression takes the form:

$$\boldsymbol{C}_{n+1}^{(\mathrm{Cont})} = \boldsymbol{C}_{n+1}^{\mathrm{vp}(\mathrm{Cont})} = K \cdot \boldsymbol{I} \otimes \boldsymbol{I} + 2G\left(\boldsymbol{I} - \frac{1}{3}\boldsymbol{I} \otimes \boldsymbol{I}\right) - 2G\gamma\hat{\boldsymbol{n}} \otimes \hat{\boldsymbol{n}}, \tag{20}$$

where $\gamma = \dfrac{1}{\dfrac{\eta}{2G\Delta t} + 1 + \dfrac{K' + H'}{3G}}$, as $\dfrac{\eta}{2G\Delta t} \to 0$, the purely plastic continuum tangent operator is obtained. Furthermore, in eq. (19), $\beta \leqslant 1$, and for a large time step $\boldsymbol{\xi}_{n+1}^{\mathrm{Tr}}$ may lay far out of the loading surface so that β may become significantly less than unity. In addition, since $\bar{\gamma} = \gamma + \beta - 1$, we have the bound $\gamma - 1 < \bar{\gamma} \leqslant \gamma$. Hence, for large time steps, eq. (19) may differ significantly from eq. (20). As a result, use of eq. (20) leads to loss of the quadratic rate of asymptotic convergence which characterizes Newton's iteration method, which represents both

more CPU time and iteration steps. It should be indicated that when $\boldsymbol{\sigma}_{n+1} = \boldsymbol{\sigma}(\boldsymbol{\varepsilon}_n, \boldsymbol{\sigma}_n, \boldsymbol{q}_n, \Delta\boldsymbol{\varepsilon}_n)$ is elastic, one has $\boldsymbol{C}_{n+1} = \boldsymbol{C}^{\mathrm{vp}}_{n+1} = \boldsymbol{C}$, where $\boldsymbol{C}$ is the fourth-order tensor of elastic constants.

3 The elasto-viscoplastic CTO based BEM

Without consideration of body force, the basic equation of BEM can be written as follows.

3.1 Elasto-viscoplastic boundary integral equation

$$\int_{\partial\Omega} [\dot{u}_i(z) - \dot{u}_i(x)] P_{ki}(x,z)\mathrm{d}S_z - \int_{\partial\Omega} \dot{p}_i(z) U_{ki}(x,z)\mathrm{d}S_z = \int_{\Omega} U_{ki,j}(x,z) C_{ijab} \dot{\varepsilon}^{\mathrm{vp}}_{ab}(z)\mathrm{d}V_z, \tag{21}$$

where x is a source point, z is a field point, U_{ki}, P_{ki} denote the components of the Kelvin fundamental displacement and traction. $\dot{\boldsymbol{u}}$ is the displacement rate vector, $\dot{\boldsymbol{p}} = \dot{\boldsymbol{\sigma}} \cdot \boldsymbol{n}$ is the traction rate vector, and the fourth order tensor $\boldsymbol{C}_{ijab}$ is elastic constant (i.e. $\boldsymbol{C}$).

In matrix form, the above BIE symbolically reads:

$$[\boldsymbol{H}]\{\dot{\boldsymbol{u}}\} - [\boldsymbol{G}]\{\dot{\boldsymbol{p}}\} = [\boldsymbol{Q}]\{\boldsymbol{C}: \dot{\boldsymbol{\varepsilon}}^{\mathrm{vp}}\}, \tag{22}$$

where $[\boldsymbol{H}]$ and $[\boldsymbol{G}]$ correspond to the matrices of elastic problem, $[\boldsymbol{Q}]$ relates to the matrix associated to nonlinear strain rate term.

In the standard boundary element method, eq. (22) is discretized and then rewritten as

$$[\boldsymbol{A}]\{\dot{\boldsymbol{y}}\} = \{\dot{\boldsymbol{f}}\} + [\boldsymbol{Q}]\{\boldsymbol{C}: \dot{\boldsymbol{\varepsilon}}^{\mathrm{vp}}\}, \tag{23}$$

where $\{\dot{\boldsymbol{y}}\}$ collects all the boundary unknowns, $[\boldsymbol{A}]$ denotes the system matrix related to the boundary unknowns and $\{\dot{f}\}$ is the contribution of known boundary variables.

3.2 Elastic-viscoplastic strain equation at internal points

Differentiation of the interior displacement rate integral equation with respect to x_l yields the representation formula for the displacement rate gradient

$$\begin{aligned}\dot{u}_{k,l}(x) = &\int_{\partial\Omega} \dot{u}_i(z) D_{kil}(x,z)\mathrm{d}S_z - \int_{\partial\Omega} \dot{p}_i U_{ki,l}(x,z)\mathrm{d}S_z \\ &- C_{ijab}\dot{\varepsilon}^{\mathrm{vp}}_{ij}(x)\int_{\partial\Omega} n_l(z) U_{ka,b}(x,z)\mathrm{d}S_z \\ &- \int_{\Omega} U_{ki,jl}(x,z) C_{ijab}[\dot{\varepsilon}^{\mathrm{vp}}_{ab}(z) - \dot{\varepsilon}^{\mathrm{vp}}_{ab}(x)]\mathrm{d}V_z,\end{aligned} \tag{24}$$

with the notation $D_{kil} = C_{ijab} n_j U_{ka,bl}$.

The strain rate equation at x is then readily obtained from eq. (24). In symbolic form, one has

$$\{\dot{\boldsymbol{\varepsilon}}\} = [\boldsymbol{G}']\{\dot{\boldsymbol{p}}\} - [\boldsymbol{H}']\{\dot{\boldsymbol{u}}\} + [\boldsymbol{Q}']\{\boldsymbol{C}:\dot{\boldsymbol{\varepsilon}}^{\mathrm{vp}}\} = -[\boldsymbol{A}']\{\dot{\boldsymbol{y}}\} + \{\dot{\boldsymbol{f}}'\} + [\boldsymbol{Q}']\{\boldsymbol{C}: \dot{\boldsymbol{\varepsilon}}^{\mathrm{vp}}\}, \tag{25}$$

where $[\boldsymbol{H}']$ and $[\boldsymbol{G}']$ are matrices related to displacement and traction rate terms, respectively; $[\boldsymbol{A}']$ is the system matrix related to boundary unknowns, $[\boldsymbol{Q}']$ corresponds to the contributions of nonlinear strain term, and $\{\dot{\boldsymbol{f}}'\}$ depends on the prescribed terms of tractions and boundary displacements.

Substituting $\{\dot{\boldsymbol{y}}\}$ from eq. (23) into eq. (25), we have

$$\{\dot{\boldsymbol{\varepsilon}}\} = \{\dot{\boldsymbol{n}}\} + [\boldsymbol{S}]\{\boldsymbol{C}:\dot{\boldsymbol{\varepsilon}}^{\mathrm{vp}}\}, \tag{26}$$

where

$$\{\dot{\boldsymbol{n}}\} = \{\dot{\boldsymbol{f}}'\} - [\boldsymbol{A}'][\boldsymbol{A}]^{-1}[\dot{\boldsymbol{f}}],\ \{\boldsymbol{S}\} = \{\boldsymbol{Q}'\} - [\boldsymbol{A}'][\boldsymbol{A}]^{-1}[\boldsymbol{Q}].$$

From eqs. (26) and (5), removing $\{\boldsymbol{C}:\dot{\boldsymbol{\varepsilon}}^{vp}\}$, the following can be obtained:

$$[\boldsymbol{S}]\{\dot{\boldsymbol{\sigma}} - \boldsymbol{C}\dot{\boldsymbol{\varepsilon}}\} - \{\dot{\boldsymbol{n}}\} + [\boldsymbol{I}]\{\dot{\boldsymbol{\varepsilon}}\} = \{\boldsymbol{0}\}. \tag{27}$$

Eq. (27) is the basic equation for developing CTO BEM. Actually it has implicitly included the equilibrium equation.

3.3 Elasto-viscoplastic CTO based boundary integral equation

Considering the increment form of eq. (27) in $\Delta t_n = t_{n+1} - t_n$:

$$[S]\{\Delta\sigma_n - C\Delta\boldsymbol{\varepsilon}_n\} - \{\Delta\boldsymbol{n}_n\} + [\boldsymbol{I}]\{\Delta\boldsymbol{\varepsilon}_n\} = \{\boldsymbol{0}\}; \tag{28}$$

on the other hand, the viscoplastic RRA eq. (6), combining the constitutive and equilibrium equations, can be written in the form

$$\{\bar{\boldsymbol{\sigma}}\} = \{\boldsymbol{\sigma}_{n+1}\} = \{\boldsymbol{\sigma}_n\} + \{\Delta\boldsymbol{\sigma}_n\}. \tag{29}$$

Inserting eq. (29) into eq. (28), the following can be obtained:

$$\{G(\Delta\varepsilon_n)\} \equiv [\boldsymbol{S}]\{\boldsymbol{\sigma}_{n+1}(\boldsymbol{\varepsilon}_n, \boldsymbol{\sigma}_n, \boldsymbol{q}_n, \Delta\boldsymbol{\varepsilon}_n) - \boldsymbol{\sigma}_n - \boldsymbol{C}\Delta\boldsymbol{\varepsilon}_n\} - \{\Delta\boldsymbol{n}_n\} + [\boldsymbol{I}]\{\Delta\boldsymbol{\varepsilon}_n\} = \{0\}, \tag{30}$$

where $G(\Delta\boldsymbol{\varepsilon}_n)$ is the residual of eq. (28) due to the RRA. The Newton method can also be applied to this case for eq. (30)

$$\Delta\boldsymbol{\varepsilon}_n^{i+1} = \Delta\boldsymbol{\varepsilon}_n^{i} - \frac{G(\Delta\boldsymbol{\varepsilon}_n^{i})}{G'(\Delta\boldsymbol{\varepsilon}_n^{i})}, \tag{31}$$

where "$'$" is the differentiation of $G(\Delta\boldsymbol{\varepsilon}_n^i)$ with respect to $\Delta\boldsymbol{\varepsilon}_n^i$.

Note the definition of CTO (18) and introduce $\delta\boldsymbol{\varepsilon}_n^i = \Delta\boldsymbol{\varepsilon}_n^{i+1} - \Delta\boldsymbol{\varepsilon}_n^i$. Finally, eq. (31) solves

$$([\boldsymbol{S}][\boldsymbol{C} - \boldsymbol{C}_{n+1}^{vp(i)}] - [\boldsymbol{I}])\{\delta\boldsymbol{\varepsilon}_n^i\} = \{G(\Delta\boldsymbol{\varepsilon}_n^i)\}, \tag{32}$$

where $\boldsymbol{C}_{n+1}^{vp(i)}$ is the elasto-viscoplastic CTO, $[\boldsymbol{S}][\boldsymbol{C} - \boldsymbol{C}_{n+1}^{vp(i)}] - [\boldsymbol{I}]$ is referred to as the global CTO[6].

The Newton step, eq. (32), involves the difference $[\boldsymbol{C} - \boldsymbol{C}_{n+1}^{vp(i)}]$ between the elastic constitutive law and the local CTO, rather than the local CTO itself. This is consistent with the fact that eq. (28) accounts for both equilibrium and elastic constitutive law, while for the FEM[2], only equilibrium is accounted for. It is convenient to solve the Newton step (32) using a block decomposition method. Once the nonlinear eq. (32) is solved for $\Delta\varepsilon_n$, the total strain and stress fields can be obtained.

Note that $[\boldsymbol{C} - \boldsymbol{C}_{n+1}^{vp(i)}] \equiv 0$ for elastic problem, which means that there exists $[\boldsymbol{C} - \boldsymbol{C}_{n+1}^{vp(i)}]$ only when the viscoplastic deformation happens. Hence, it is convenient to rewrite the Newton step, eq. (32) using a block decomposition:

$$\begin{aligned} ([\boldsymbol{S}][\boldsymbol{C} - \boldsymbol{C}_{n+1}^{vp(i)}] - [\boldsymbol{I}])_{vpvp}\{\delta\boldsymbol{\varepsilon}_n^i\}_{vp} &= \{G(\Delta\boldsymbol{\varepsilon}_n^i)\}_{vp}, \\ \{\delta\boldsymbol{\varepsilon}_n^i\}_e &= ([\boldsymbol{S}][\boldsymbol{C} - \boldsymbol{C}_{n+1}^{vp(i)}])_{evp}\{\delta\boldsymbol{\varepsilon}_n^i\}_{vp} - \{G(\Delta\boldsymbol{\varepsilon}_n^i)\}_e, \end{aligned} \tag{33}$$

where the subscripts e and vp indicate vectors and matrices restricted to the currently elastic or viscoplastic nodes and collocation points. This shows that the global CTO has to be set up and factored only at currently viscoplastic nodes, the currently elastic part $\{\delta\boldsymbol{\varepsilon}_n^i\}_e$ being given explicitly by the second equation of eq. (33), after the first equation of (33) is solved for $\{\delta\boldsymbol{\varepsilon}_n^i\}_{vp}$. Moreover,

$$([\boldsymbol{S}][\boldsymbol{C} - \boldsymbol{C}_{n+1}^{vp(i)}])_{vpe} = ([\boldsymbol{S}][\boldsymbol{C} - \boldsymbol{C}_{n+1}^{vp(i)}])_{ee} = [0]. \tag{34}$$

Eq. (34) shows that the dimension of the linear system in eq. (33) is directly associated to the size of the plastic deformation zone. The leads to an efficient solution scheme with savings in computing time, which is different from FEM.

4 Algorithm

The following algorithm based on the above sections is proposed for solving the incremental elasto-viscoplastic problem, from initial time t_0 to final time t_{N_T}, N_T is the total load steps. The initial time t_0 is assumed to correspond to the first yield load.

For $n \in [0,\ N_T - 1]$:

1. compute $\{\Delta \boldsymbol{n}_n\}$ (purely elastic internal strain).

2. Initialize $\{\Delta \boldsymbol{\varepsilon}_n^0\}$ (e.g. to the elastic value).

iterative solution:

(a) $i = 0$.

(b) Compute the residual $\{G(\Delta \boldsymbol{\varepsilon}_n^i)\}$ from eq. (30).

(c) Convergence test: if $\| \{G(\Delta \boldsymbol{\varepsilon}_n^i)\} \| \leqslant \mathrm{Tol}$, Tol is given tolerance, then start new load increment (go to 3).

(d) $i = i + 1$.

(e) Compute the converged $[\dot{\gamma} \Delta t]$ and the local CTO $\boldsymbol{C}_{n+1}^{\mathrm{vp}(i)}$ at all nodes; determine the sets of currently elastic (e) and currently viscoplastic (vp) nodes.

(f) Set up global CTO $[\boldsymbol{S}(\boldsymbol{C} - \boldsymbol{C}_{n+1}^{\mathrm{vp}(i)}) - \boldsymbol{I}]$ and factor it into $[\boldsymbol{S}(\boldsymbol{C} - \boldsymbol{C}_{n+1}^{\mathrm{vp}(i)}) - \boldsymbol{I}]_{\mathrm{vpvp}}$ and $[\boldsymbol{S}(\boldsymbol{C} - \boldsymbol{C}_{n+1}^{\mathrm{vp}(i)}) - \boldsymbol{I}]_{\mathrm{evp}}$.

(g) Solve the first equation of eq. (33) for $\{\delta \boldsymbol{\varepsilon}_n^i\}_{\mathrm{vp}}$ and then compute $\{\delta \boldsymbol{\varepsilon}_n^i\}_{\mathrm{e}}$ using the second equation.

(h) Update: $\{\Delta \varepsilon_n^{i+1}\} = \{\Delta \varepsilon_n^i\} + \{\delta \varepsilon_n^i\}$.

(i) Start new iteration (at step (b)).

3. Update: $\{\bar{e}^{\mathrm{vp}}\}_{n+1} = \{\bar{e}^{\mathrm{vp}}\}_n + \sqrt{\frac{2}{3}}[\dot{\gamma} \Delta t]$, $\{\boldsymbol{\sigma}_{n+1}\} = \{\bar{\boldsymbol{\sigma}}(\Delta \boldsymbol{\varepsilon}_{n+1}^i)\}$, $\{\boldsymbol{\varepsilon}_{n+1}\} = \{\boldsymbol{\varepsilon}_n\} + \{\Delta \boldsymbol{\varepsilon}_n\}$.

Repeat the above process until the prescribed load, where the load is a generalized load, it may be the traction or displacement.

5 Numerical examples

A boundary element program has been developed to perrform general elasto-viscoplastic analysis of two-dimensional problems. Quadratic elements are used for both boundary and domain discretization. Corners have been modeled by means of double nodes. The following two examples have been investigated, one is a hollow specimen under uniform prescribed tension displacement. The other is a hollow cylinder subjected to internal pressure. All examples are computed at the SGI Work Station, University of California, Davis, USA.

5.1 A hollow specimen under uniform prescribed displacement

This example is taken from Ibrahimbegovic et al.[5]. We try to make comparison of the viscoplastic CTO BEM formulations with the latest FEM results obtained by Ibrahimbegovic et al. The material constants are chosen with Young's modulus $E = 70$, and Poisson's ratio $\nu = 0.2$,

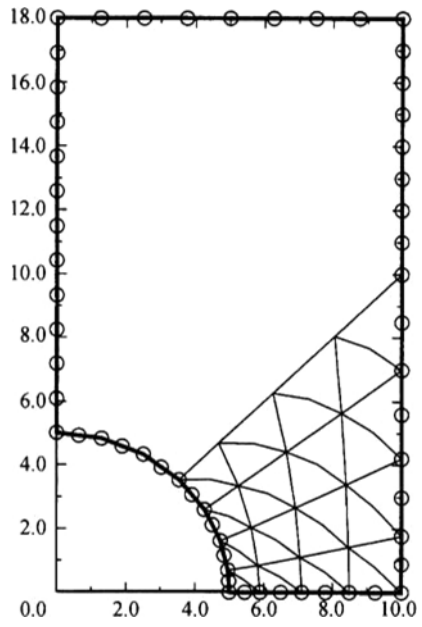

Fig. 2. BEM mesh for analysis of a hollow specimen under uniform prescribed displacement at the top. The boundary discretization consists of 29 quadratic boundary elements and 63 nodes (including 5 double nodes for the corners); the domain discretization consists of 32 cells (T6) and 81 nodes.

the kinematic hardening with modulus $H' = 0.15$, and the isotropic hardening rule of exponential type is taken from the saturation type of yield condition, $\bar{\kappa} = (\sigma_\infty - \sigma_y)(1.0 - e^{-\beta \bar{e}^{vp}}) + K\bar{e}^{vp}$, and the yield function $\kappa = \sigma_y + \bar{\kappa}$, where the saturation stress σ_∞ and the initial yield stress σ_y and related parameters are taken as

$\sigma_\infty = 0.343$, $\sigma_y = 0.243$, $K = 0.15$, $\beta = 0.1$.

(Note: Ref. [6] did not indicate the units in the example, that is the so-called unified dimension)

Two different values of viscoplastic parameters are considered to be $\eta = 0.1$ and $\eta = 10.0$. The convergence tolerance is taken to be 5.0×10^{-10}. The analysis is performed by imposing the prescribed displacement of $U_1 = 0.1$ (acts on the top side of the sample). The final displacement value is reached in ten time steps, each one being equal to $\Delta t = 0.01$. Due to the symmetry of the sample, only one quarter of the specimen is modeled by using 29 quadratic boundary elements and 32 quadratic triangular internal cells (T6) (see fig. 2). It has a hole with inner radius 5, length side is 18 and width side is 10. The calculated results are shown in fig. 3. Fig. 3 gives the comparison of load-displacement diagrams for $\eta = 0.1$ and $\eta = 10.0$. From fig. 3 we can see that the results of the two methods agree very well, which shows the effectiveness and accuracy of the viscoplastic CTO BEM.

5.2 A thick walled cylinder under internal pressure

This example uses the results of ABAQUS for comparison since there is no analytical solution under the Von-Mises yield condition. The related material constants are chosen as:

shear modulus $G = 1.0$ Pa, $\nu = 0.3$, $H' = 0.0$, $\eta = 0.0$, 10^{-3}, 10^{-2}, 10^{-1}, 1.0, 10^2, 10^3(MPa · h), $\kappa = 2G(0.001 + 0.001(\bar{e}^{vp})^m$, in which $m = 0.2$. The converged tolerance is still taken to be 5.0×10^{-10}, $p = 12.0 \times 10^{-4}$(MPa), is applied with one load step and $\Delta t = 0.1$ (h).

The thick walled cylinder has inner radius $a = 1$ m and outer radius $b = 2$ m. The sample is modeled with one quarter due to the

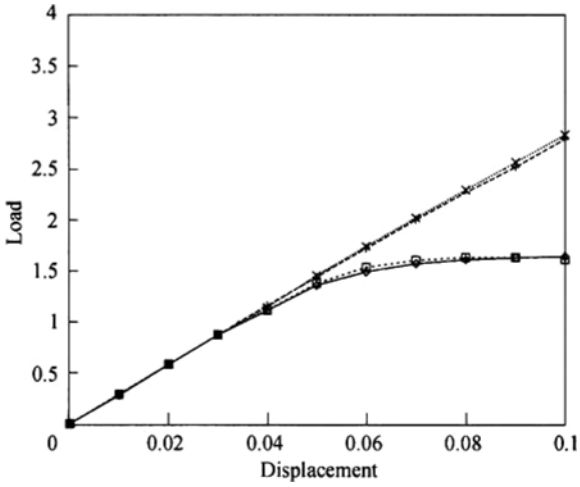

Fig. 3. Comparison of load-displacement diagrams for η(ETA) = 0.1 and η(ETA) = 10. ◇, ETA = 0.1[5]; +, ETA = 10[5]; □, ETA = 0.1; ×, ETA = 1.0.

symmetry. The mesh is shown in fig. 4. In FEM-ABAQUS, 100 8-noded quadrilateral cells are introduced. The computed results are shown in figs. 5 and 6 and table 1. Due to the lack of the viscoplastic material model in ABAQUS, only the elastic and elastoplastic solutions are presented as the comparison of limit cases in elasto-viscoplasticity. Fig. 5 gives the comparison of hoop stresses with different viscoplastic fluidity parameters along the radius and ABAQUS solutions in pure elasticity and plasticity. Fig. 6 shows the hoop stress at inner radius $a = 1$ m varies with time in three viscoplastic fluidity parameters. Table 1 shows the iterations, CPU times and norm errors with different viscoplastic parameter η.

From fig. 5, one can see that as $\eta \to 0$, the result is very close to ABAQUS plastic solution; as

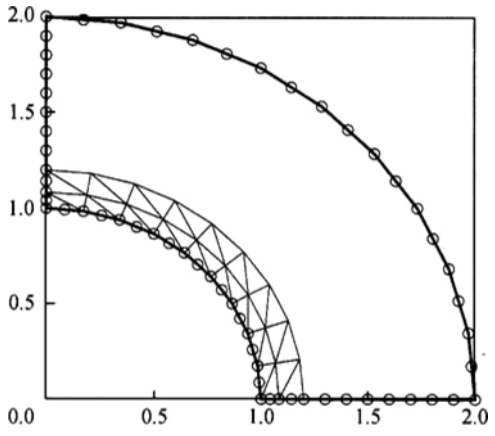

Fig. 4. BEM mesh for analysis of the hollow cyclinder under pressure. The boundary discretization consists of 30 quadratic boundary elements and 64 nodes (including 4 double nodes for the corners); the domain discretization consists of 36 cells (T6) and 81 nodes.

Table 1 Number of iterations, CPU time and residual norm for various viscoplastic parameters η

η/MPa·h	Δt/h	Iterations	CPU time/s	Norm errors
0.0	0.1	3	41.89	3.030×10^{-11}
10^{-3}	0.1	3	41.84	3.169×10^{-11}
10^{-2}	0.1	3	41.83	3.218×10^{-11}
10^{-1}	0.1	3	42.70	3.674×10^{-11}
1.0	0.1	2	39.45	2.554×10^{-11}
10^{2}	0.1	1	39.93	2.697×10^{-11}
10^{8}	0.1	0	33.31	1.999×10^{-11}

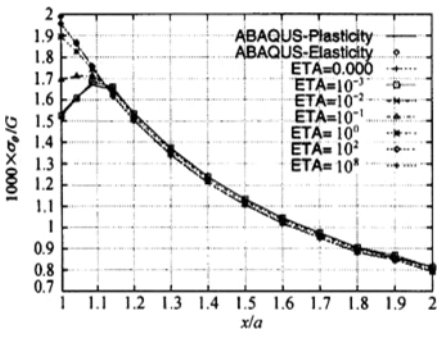

Fig. 5. Comparison of hoop stresses with different viscoplastic fluidity parameters (η = ETA) along radius.

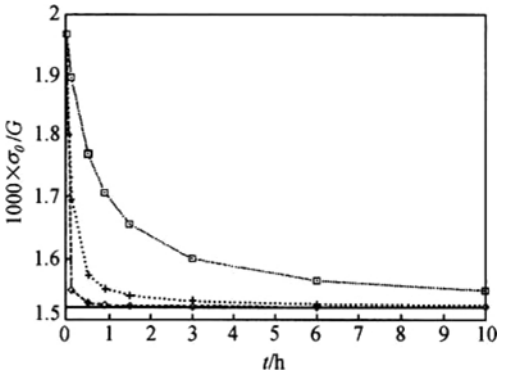

Fig. 6. Hoop stresses at inner radius 1 versus time in three viscoplastic fluidity parameters (η = ETA). —, ABAQUS-plasticity; ◇, ETA = 0.01; +, ETA = 0.1; □, ETA = 1.0.

$\eta \to \infty$ ($\eta = 10^8$ MPa·h), the results reach the ABAQUS purely elastic solution, and all the results with different $\eta = 10^{-3}$, 10^{-2}, 10^{-1}, 1.0, 10^2(MPa·h) are located within the limit solutions of $\eta = 0$ (MPa·h) and $\eta = 10^8$(MPa·h). From fig. 6, it can be seen that as $t \to \infty$, all the three solutions approach the pure plastic solution. This limiting process is the so-called viscoplastic steady state approaching solution. In addition, the viscoplastic fluidity parameter η affects the stress decaying properties. The larger the values of η are, the less the decaying the stresses appear to be.

6 Conclusions

This paper presents a CTO-based BEM for elasto-viscoplastic deformation problems. The viscoplastic RRA and CTO are developed for nonlinear BEM. Both kinematic and isotropic strain hardening are considered. Two numerical examples with different viscoplastic fluidity parameters are presented and compared with the latest solutions (Ibrahimbegovic et al.) and FEM code ABAQUS. The results show that the computations of this paper and the FEM agree very well. Further, it is clearly observed that the viscoplastic fluidity parameter η affects the stress decaying properties. The larger the values of η are, the less the decaying the stress appears to have.

The numerical results support the fact that the viscoplastic solutions approach two limit cases, i.e. the pure elastic solution as $\eta \to \infty$ and rate-independent plastic solution as $\eta \to 0$. In addition, as $t \to \infty$, the viscoplastic steady state solution is reached, which is just the rate-independent plastic solution. These results agree with the theory of elasto-viscoplasticity.

Acknowledgements The first author particularly thanks Dr. S. Mukherjee and Dr. H. Poon of Cornell University for their helpful discussion and help. This work was supported by the Zhejiang Natural Science Foundation Special Funds (Grant No. Rc. 9601) and US National Science Foundation (NSF) (Grant No. CNS-9713008).

References

1. Simo, J. C., Taylor, R. L., Consistent tangent operators for rate-independent elastoplasticity, Comput. Methods Appl. Meth. Eng., 1985, 48: 101.
2. Simo, J. C., Hughes, T. J. R., Computational Inelasticity, New York: Springer-Verlag, 1998.
3. Vidal, C. A., Lee, H. S., Haber, R. B., The consistent tangent operator for design sensitivity of history-dependent response, Comp. Syst. Eng., 1991, 2: 509.
4. Vidal, C. A., Haber, R. B., Design sensitivity analysis for rate-independent elasto-plasticity, Comput. Methods Appl. Mech. Eng., 1993, 107: 393.
5. Ibrahimbegovic, A., Gharzeddine, F., Chorfi, L., Classical plasticity and viscoplasticity models reformulated: Theoretical basis and numerical implementation, Int. J. Numer. Methods Eng., 1998, 42: 1499.
6. Bonnet, M., Mukherjee, S., Implicit BEM formulations for usual and sensitivity problems in elastoplasticity using the CTO concept, Int. J. Solids Struct., 1996, 33: 4461.
7. Poon, H., Mukherjee, S., Bonnet, M., Numerical implementation of a CTO-based implicit approach for the BEM solution of usual and sensitivity problems in elastoplasticity, Eng. Anal. Boundary Elem., 1998, 22(4): 267.
8. Bonnet, M., Poon, H., Mukherjee, S., Hypersingular formulation for boundary strain evaluation in the context of a CTO-based implicit BEM scheme for small strain elastoplasticity, Int. J. Plasticity, 1998, 14(10-11): 1033.
9. Paulino, G. H., Liu, Y., Implicit consistent and continuum tangent operators in elastoplastic boundary element formulations, Comput. Methods. Appl. Mech. Eng. (to be published).
10. Perzyna, P., Thermodynamic theory of viscoplasticity, Adv. Appl. Mech., 1971, 11: 313.